BNL-224483-2023-JAAM

Solution-Processable Copper Halide Based Hybrid Materials Consisting of Cationic Ligands with Different Coordination Modes

X. Hei, M. Li

To be published in "Inorganic Chemistry"

February 2023

Center for Functional Nanomaterials

Brookhaven National Laboratory

U.S. Department of Energy

USDOE Office of Science (SC), Basic Energy Sciences (BES) (SC-22)

DISCLAIMER

Solution–Processable Copper Halide Based Hybrid Materials Consisting of Cationic Ligands with Different Coordination Modes

Xiuze Hei, [a] Simon J. Teat, [b] Mingxing Li, [c] Megan Bonite, [a] Jing Li*[a]

[a] *Department of Chemistry and Chemical Biology, Rutgers University, Piscataway, New Jersey 08854, USA. E-mail: jingli@rutgers.edu.*
[b] *Advanced Light Source, Lawrence Berkeley National Laboratory, Berkeley, CA 94720, USA.*
[c] *Center for Functional Nanomaterials, Brookhaven National Laboratory, Upton, NY, 11973, USA.*

ABSTRACT: Using cationic ligands containing both aromatic and aliphatic coordination sites, we have synthesized and structurally characterized five new CuX–based hybrid materials consisting of anionic inorganic motifs that are also form coordinate bonds with the cationic organic ligands. As a result of the unique bonding nature at the inorganic/organic interfaces, these compounds demonstrate strong resistance towards heat and can be readily processed in the solution. They emit light in the visible region ranging from cyan to yellow color, with the highest PLQY reaching 71%. The influence of the different coordination modes of the ligands on their emission behavior was investigated employing both experimental and theoretical methods, which have provided insight in understanding structure–property relationships in these materials and guidelines for tuning and enhancing their chemical and physical properties.

Introduction

Crystalline inorganic–organic hybrid semiconductors have continued to attract great attention due to their potential in clean energy related applications, including, but not limited to, solid–state lighting (SSL)[1-3], photovoltaics (PV)[4-5], and luminescent solar concentrators (LSC).[6-7] These materials possess a wide range of interesting properties that can be finely tuned by varying their organic and/or inorganic modules.[8-9] Intriguingly, not only the existing properties inherent to their inorganic or organic components, but also new properties that are extrinsic to either counterpart are often observed in these hybrid materials, as a result of the unique bonding characteristics at their inorganic/organic interfaces.[10-13]

One of the most interesting hybrid material families consists of copper(I) halides. This material family demonstrate remarkable structural diversities and facile synthesis, coupled with excellent luminescent properties and robustness, and have been well-recognized as promising functional materials for light–emission related applications.[14-17] The CuI–based hybrid materials can be classified into three subgroups based on the types of chemical

bonds between their inorganic and organic counterparts, namely, structures built on pure coordinate bonds (Subgroup 1), structures made of pure ionic bonds (Subgroup 2), and structures composed of both ionic and coordinate bonds (Subgroup 3) or All-in-one (AIO) structures.[11, 18-20] Among the three subgroups, the AIO structures are of particular interest due to their interesting and unique bonding characteristics. A typical AIO structure consists of anionic inorganic $(Cu_mI_{m+n})^{n-}$ modules and cationic organic ligands L^{k+} (k = 1, 2), which are further connected via dative Cu–L bonds to form an overall charge–neutral compound. This interesting approach successfully blends the coordination bonds (as in Subgroup 1 structures) and ionic bonds (as in Subgroup 2 structures) at the inorganic/organic interfaces, thus providing the AIO structures with all beneficial features from the two subgroup compounds. These include optical tunability, strong luminescence, solution processability and framework stability.[19, 21-23] All of these desirable features give the AIO compounds preference for use in solution–processed thin film devices, thus broadening their applications.

To obtain AIO structures, ligands are designed to contain both a cationic center (e. g. quaternary N or P atoms) to form ionic bonds with anionic inorganic modules $(Cu_mI_{m+n})^{n-}$, and free binding sites for subsequential coordination to Cu atoms. Depending on the hybridization of the coordinative atoms, sp^3 for aliphatic binding sites or sp^2 for aromatic binding sites, the AIO compounds so formed may follow different emission mechanisms. Ligands with aliphatic binding sites [e.g., N-monoalkylated TEDs (triethylenediamine)] have gained attention as low-cost and efficient cationic ligands for the construction of AIO structures with high photoluminescence quantum yields (PLQYs) and good thermal stability.[6, 19, 24] However, due to the lack of ligand π^* states to participate in the emissive transition and the relatively close Cu···Cu distance (< 2.80 Å, twice the vdW radius of Cu atom), their photoluminescence is typically a cluster-centered (CC) emission.[11, 18, 25] Therefore, their emission energies are mainly determined by the inorganic modules with limited ligand effect, making it difficult to tune the emission color. On the other hand, Ligands with aromatic binding sites generally afford AIO structures that follow a metal/halide-to-ligand charge transfer [(M+X)LCT] emission mechanism, which allows the systematic regulation of emission energy by adjusting the lowest unoccupied molecular orbital (LUMO) energies of the ligands.[23] But such structures usually have relatively lower decomposition temperatures, as a result of relatively weaker coordination strength compared to that of TED.

Herein, we design and synthesize a series of cationic ligands with both aromatic and aliphatic coordination sites. Reactions of these ligands with CuI led to five new AIO compounds ranging from 0D molecular species to 2D extended network. Compounds with ligands of different coordination modes (i.e., via aliphatic N and/or aromatic N) were identified. All compounds demonstrate good thermal stability with decomposition temperature at 210 °C or higher. Their emission maximum ranges from 470 nm to 555 nm with highest PLQY reaching 71%. The emission mechanisms of these compounds were

studied by both experimental and theoretical methods. The results clearly suggest that ligand configuration plays an important role in the emission properties of the resultant hybrid structures. Such studies have provided insight into the better understanding of structure–property relationships of CuX–based hybrid materials.

Results and Discussions

Structural Description. The cationic ligands were synthesized by a two-step process (Fig. 1a). First, alkylation occurred on the NH site of a N–heterocyclic ring leaving aromatic N atom available for the subsequent coordination to Cu metal. The alkylated species was then reacted with TED by Menshutkin reaction,[26] yielding ammonium as a cationic center, as well as a coordination available aliphatic N atom. The molecular structures of these ligands are shown in Figs. S1-4 along with 1H NMR spectra to confirm their purity. All the ligands have not been reported before. As an efficient method for obtaining high-quality single crystals of CuI–based structures, the layered diffusion method was used to synthesize single crystals of all five compounds suitable for single-crystal X-ray analysis.[27-28] (Fig. S8) Their structures are depicted in Figs. 1b-f and Fig. S6. They are identified as 0D-$Cu_4I_6(L_1)_2$ (**1**), 0D-$Cu_4I_6(L_2)_2$ (**2**), 0D-$Cu_2I_4(L_2)_2$ (**3**), 1D-$Cu_6I_8(L_3)_2$ (**4**) and 2D-$Cu_4I_6(L_4)_2$ (**5**). Direct coordination between anionic inorganic motifs and cationic ligands are observed in all title compounds, thus giving overall charge neutral AIO compounds. The phase purity was confirmed by powder X-Ray diffraction (PXRD) analysis as shown in Fig. 1g.

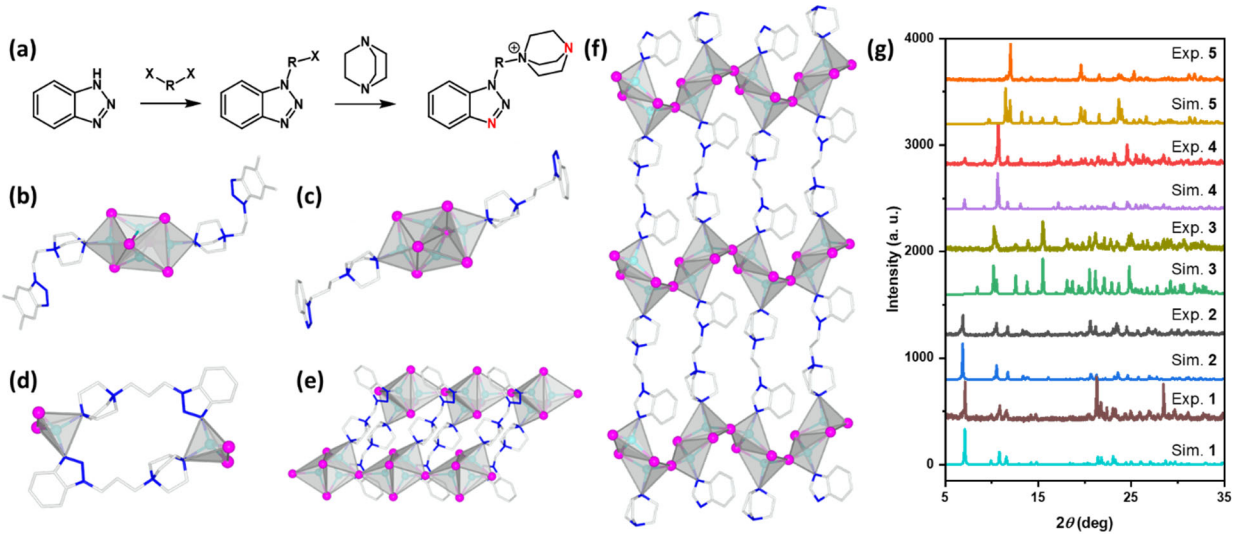

Figure 1. (a) Synthetic approach used to prepare cationic ligands with free N binding sites marked in red. X = Cl, Br, or I. Crystal structures of compounds (b) **1**, (c) **2**, (d) **3**, (e) **4**, and (f) **5**. Color scheme: cyan: Cu; purple: I; gray: C; blue: N. All H atoms, disorders and solvated molecules are omitted for clarity. (g) PXRD patterns of all compounds.

Compounds **1** and **2** share the same type of structure, namely oD-$Cu_4I_6^{2-}$ clusters coordinated to two terminal ligands. Only the aliphatic N atoms are involved in the Cu-N coordination. The same inorganic motif has been observed in other AIO compounds made with TED containing ligands, indicating the structural directing effect of this specific bind site. Their shortest Cu···Cu distances are 2.68 Å and 2.57 Å, respectively. As these values are shorter than twice the vdW radius of Cu atom (2.80 Å),[29] strong cuprophilic interactions (the closed-shell d^{10}–d^{10} Cu^I–Cu^I interactions) may exist within these structures.

Table. 1 Summary of crystallographic data of compounds **1–5**.

Compound	**oD-$Cu_4I_6(L_1)_2$ (1)**	**oD-$Cu_4I_6(L_2)_2$ (2)**	**oD-$Cu_2I_4(L_2)_2$ (3)**	**1D-$Cu_6I_8(L_3)_2$ (4)**	**2D-$Cu_4I_6(L_4)_2$ (5)**
Crystal System	triclinic	monoclinic	monoclinic	monoclinic	monoclinic
Empirical Formula	$C_{32}H_{48}Cu_4I_6N_{10}$	$C_{30}H_{44}Cu_4I_6N_{10}$	$C_{30}H_{44}Cu_2I_4N_{10}$	$C_{13}H_{18}Cu_3I_4N_5$	$C_{15}H_{21}Cu_2I_3N_4$
FW	1588.36	1566.12	1179.43	942.54	765.14
Space Group	*P* -1	*C* 2/c	*P* 2_1/n	*P* 2_1/c	*P* 2_1/n
a (Å)	9.6591(11)	27.6248(9)	11.6522(13)	6.7691(6)	11.6260(12)
b (Å)	10.0200(11)	9.6289(3)	9.5069(10)	19.2536(18)	14.7894(15)
c (Å)	13.2071(15)	18.0001(6)	17.1437(18)	16.4625(16)	11.8173(12)
α (°)	88.007(4)	90	90	90	90
β (°)	71.659(4)	111.457(1)	101.437(4)	93.384(4)	100.346(4)
γ(°)	63.568(4)	90	90	90	90
V (Å^3)	1078.1(2)	4456.1(3)	1861.4(3)	2141.8(3)	1998.8(4)
Z	1	4	2	4	4
T (K)	100 (2)	100 (2)	100 (2)	100(2)	100(2)
λ(Å)	0.72880	0.72880	0.72880	0.72880	0.72880
R_1	0.0267	0.0223	0.0165	0.0201	0.0254
wR_2	0.0642	0.0474	0.0383	0.0518	0.0612

Note: One molecule of MeCN and the disorders in compound **2** were separately removed for formula consistency.

In compounds **3–5**, both coordination available N atoms, namely aromatic N from the N–heterocyclic ring and aliphatic N from TED, participate in the formation of dative bonds. Compound **3** was made of same ligand as in compound **2** but with a lower CuI/L feeding ratio. While compound **3** is a cyclic 0D molecular structure made of two CuI_2^- monomers and two 2–connected ligands, compounds **4** and **5** consist of 1D anionic CuI chains that are interconnected and charge-balanced by the ligands. The 1D-$Cu_6I_8^{2-}$ inorganic chains in compound **4** consist of Cu_3I_4 subunits linked together via μ_3–I atoms, with the shortest Cu···Cu distance of 2.61 Å (shorter than twice the vdW radius of Cu atom). Two chains are further connected by the V–shape ligands, thus forming a 1D tube-like structure of **4**. It crystalizes in a monoclinic $P2_1/c$ space group. In compound **5**, the 1D–$Cu_4I_6^{2-}$ chains are composed of Cu_2I_2 rhomboids and bridging I atoms. With the longer alkyl group, L_4 is more flexible compared to L_3, and thus tends to be more linear and leading to the formation of 2D extended structures of **5**, suggesting the fact that ligand conformation plays a role in affecting the structure. Interestingly, while an isoreticular structure has been reported with short Cu···Cu distance of 2.67 Å using pure aliphatic 2–connected ligand,[30] the shortest Cu···Cu distance in compound **5** was found to be 3.34 Å. The significant difference may suggest the effect of introducing aromatic entity.

The Cu–N bond lengths of these compounds are found to be 2.04–2.17 Å, similar to other reported AIO and Subgroup 1 CuI hybrids.[25, 28, 31-32] In all structures, Cu atoms are tetrahedrally coordinated to either iodine atoms or ligands, while the coordination number of I atoms range from 1 to 3. The important crystallographic data are summarized in Table. 1.

DFT Calculations. To understand their electronic structures, we carried out DFT calculations on all five compounds. The projected density of states (PDOS) of all title compounds were calculated using Cambridge Serial Total Energy Package (CASTEP).[33] The calculation details can be found in the experimental section. For compounds **1** and **2**, as their aromatic units (N–heterocyclic rings) are far away from the anionic $Cu_4I_6^{2-}$ clusters and spaced by alkyl chains with much higher lying energy levels, it is rational to consider them as separated components with little-to-no interactions with other parts of the compounds. Therefore, the contributions of N–heterocyclic rings were excluded from the calculated results of **1** and **2** for clarity, as depicted in Fig. 2a and Figs. S9-10. Both the valence band maximum (VBM) and conduction band minimum (CBM) of compounds **1** and **2** are primarily populated by the atomic states from the inorganic clusters, namely, Cu 3d and I 5p for VBMs and Cu 4s, Cu 4p and I 6s for CBMs. These results clearly suggest the typical CC emission nature of compounds **1** and **2**, similar to previously reported AIO structures made of N–monoalkylated TEDs.[6, 19, 24]

Interestingly, the influence of involving aromatic systems in the Cu–N coordination has been successfully captured by the calculations. The results of compounds **3-5**, in which aromatic N atoms are coordinated directly to their inorganic motifs, demonstrate different

characteristics compared to the cases in compounds **1-2**. While the main contributions to their VBMs also come from the inorganic anions (Cu 3d and I 5p orbitals), their CBMs are made of C 2p and N 2p orbitals from the cationic ligands (Fig. 2b and Figs. S11-13). The ligands contributions are dominated by the aromatic N–heterocyclic π systems. Therefore, their emission is largely associated with (M+X)LCT mechanism.[18, 28] Additionally, the higher energy region of the conduction band in compound **4** is also populated by atomic states from its inorganic motif, while for that of compound **3** such contributions is negligible. (Figs. S11-12) This may possibly be due to short Cu···Cu distance in compound **4** (2.61 Å). Since the inorganic contributions overlap with the ligand contributions at the higher energy region of conduction bands in compound **4**, it may imply the existence of CC excited state with a slightly higher energy level above the (M+X)LCT excited state, which could be activated through the (M+X)LCT states via the thermal equilibrium between these two excited states.[34] This behavior has been observed in other CuX–based hybrid materials.[14, 30]

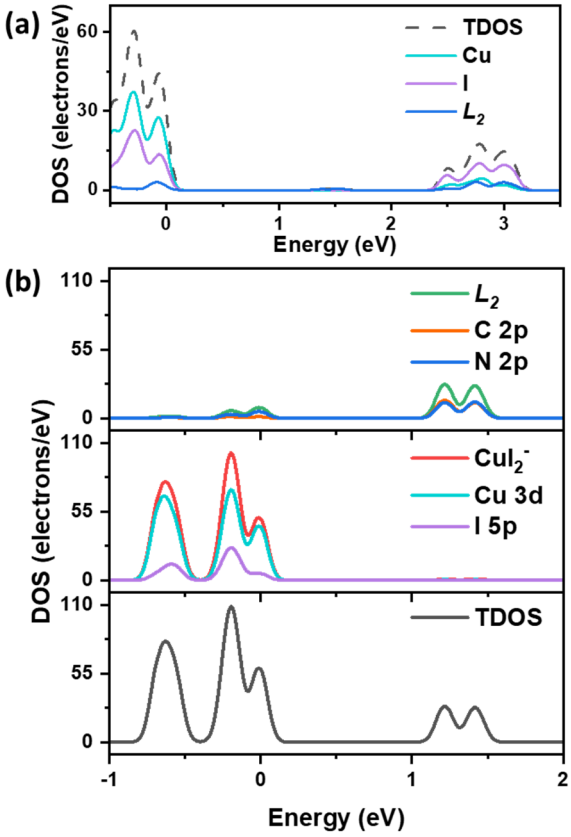

Figure 2. Calculated total density of states (TDOS) and projected density of states (PDOS) of compounds (a) **2** and (b) **3**.

Photophysical Study. The photophysical properties of all title compounds were investigated using photoluminescence spectroscopy and diffuse reflectance spectroscopy

at room temperature. The important properties are summarized in Table 2. Upon excitation, all compounds exhibit photoluminescence with emission maximum between 470 and 555 nm. Their emission colors range from cyan with Commission International del'Eclairage (CIE) color coordinates (x, y) of (0.22, 0.27) to yellow with CIE coordinates of (0.42, 0.53). The emission profiles of all title compounds demonstrate single band but broad shape with a full-width at half-maximum (FWHM) of ~120 nm. This implies that their excited states are of charge transfer characteristics, which has been observed for many CuX–based hybrid materials.[35] The excitation-dependent PL data are plotted in Figs. 3c and Fig. S14. Excluding compound **4**, all other compounds show little change in their emission wavelength and emission profile at different excitation energies, and only the changes in emission intensities were observed. This indicates that their emissions originate from a single excitation process. On the other hand, a second emission peak centered at 490 nm was observed in compound **4** when excited at higher excitation energies. This result further suggests that not only the (M+X)LCT, but also the CC excited state are involved in the radiative process of compound **4**. The optical absorption spectra of all five compounds were collected at room temperature using diffuse reflectance spectroscopy (Fig. 3d). Their bandgaps estimated from the absorption edges are 2.8, 3.0, 2.6, 2.7 and 3.4 eV, respectively, for **1-5**. The internal quantum yield (IQY) of all compounds were determined at room temperature under 360 nm excitation and the values are listed in Table 2. The three 0D molecular species, namely compounds **1-3**, demonstrate higher IQYs compared to those of compounds **4** and **5**, which consist of infinite 1D CuI anionic chains. This may be possibly due to the restricted molecular motions and less non-radiative channels in the 0D compounds.[36-38]

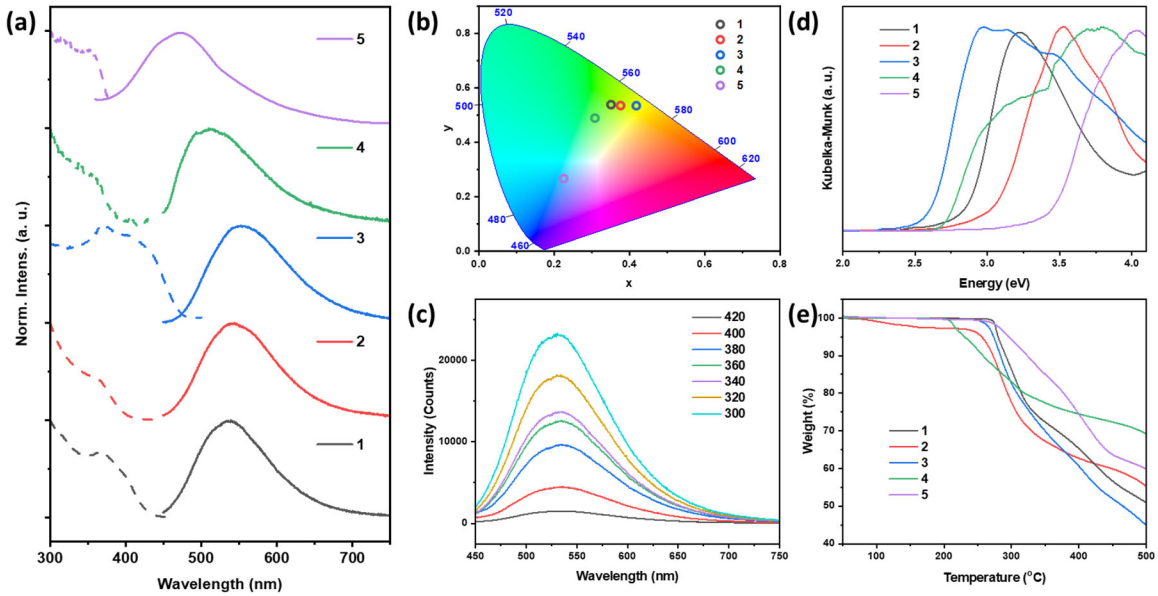

Figure 3. (a) Normalized PLE (dashed) and PL (solid) spectra and (b) color chromaticity of all five compounds. (c) Excitation-dependent PL spectra of compound **1**. (d) Optical absorption spectra and (e) TG plots of all title compounds.

Thermalgravimetric analysis (TGA) was performed to evaluate the thermal stability of all title compounds. As shown in Fig. 3e, except compound **4**, which decomposes at 210 °C, all other compounds remain stable up to 240 °C. The relatively lower thermal resistance of compound **4** may be attributed to the structural hindrance of the ligands, as the bulky functional groups are connected by a rigid $-CH_2-$ only. The weight loss between 60 to 150 °C in compound **2** (2.9%) is attributed to the loss of solvated MeCN molecules (calc. 2.7%). Above 210 °C, the weight losses are associated with the loss of organic cations.[39-40] Interestingly, compounds **2** and **3**, which are two different structures made of the same cationic ligands with different coordination modes, demonstrate similar decomposition temperatures. This suggests that the thermal stability of these compounds mainly depends on the TED part of the ligands rather than their aromatic coordination sites. Therefore, implementing aliphatic coordination groups which can form stronger Cu–N bonds leads to enhanced resistance towards heat. As a result, compound **3** demonstrates 50-70 °C higher decomposition temperature compared to some reported 0D AIO clusters made of only aromatic N-Cu bonds.[19] The structure of their inorganic motifs may also contribute to the thermal stability.

Table 2. Important photophysical properties of compounds **1–5**.

#	B. G. (eV)	λ_{em} (nm)	CIE	IQY [a] (%)	T_D [b] (°C)	Solubility [c] (mg/ml)
1	2.8	535	(0.35, 0.54)	71	270	60
2	3.0	540	(0.38, 0.54)	47	240	80
3	2.6	555	(0.42, 0.53)	54	250	80
4	2.7	512	(0.31, 0.49)	3	210	110
5	3.4	470	(0.22, 0.27)	7	260	100

[a] λ_{ex} = 360 nm; [b] T_d: decomposition temperature; [c] Test in DMSO at room temperature.

Another important and advantageous feature of AIO-type compounds is their solution processability. All title compounds demonstrate good solubility in DMSO as listed in Table 2, comparable to other AIO-type materials reported to date,[11, 22] while most Subgroup 1 CuX–based hybrid materials are insoluble in common solvents.[27, 31-32] Suggested by previous studies concerning the solvation behavior of AIO-type compounds, this intriguing phenomenon is attributed to the introduction of ionic bonds at the inorganic/organic interface.[21, 23, 41] Confirmed by the ^{1}H NMR spectrum of dissolved compound **4** (Fig. S5), the differences compared to that of free ligand *L4* I clearly suggest that the dissolved species exist as small fragments composed of anionic CuX clusters, which remain coordinated to the cationic ligands via dative bonds. As compounds **4** and **5** have more Cu atoms with relatively weaker aromatic N–Cu bonds, the generation of such soluble fragments in DMSO may be easier to occur and lead to higher solubility. Upon slow cooling or the addition of antisolvents (e.g., MeOH), these compounds can reprecipitate out from their saturated DMSO solutions and regain crystallinity, as depicted in Fig. S15.

To understand the emission mechanism, temperature–dependent PL spectroscopy and lifetime measurements were carried out on selected compounds and the results are displayed in Fig. 4 and Figs. S15-17. Compound **2**, in which only the aliphatic part of the ligand coordinates to the inorganic cluster, exhibits thermochromic behavior. Upon increasing temperature, a small red shift of the major peak was observed, accompanied by the emergence of a shoulder peak at around 600 nm (Fig. 4a and Fig. S16). While the shift of the major peak can be attributed to increased localization of the excited state and reduced structural torsion at relatively lower temperatures, the appearance of shoulder peaks clearly suggests there is another radiative decay pathway. Accordingly, the PL decay curves of compound **2** at various temperatures are best fit with a biexponential function (Table S1). The decrease of the fast decay lifetimes from 5.3 μs to 1.2 μs from 78 K to 300 K, is attributed to the phosphorescence arising from the CC excited states, and is similar to those observed in the 0D AIO-type structures made of N–monoalkylated TEDs.[6, 19] The slow decay lifetimes range from 22.3 μs (78 K) to 12.4 μs (300 K) with their fractions increasing

from 11.6% (78 K) to 36.1% (300 K). As this decay pathway is insensitive to excitation energy changes (Fig. S14), they are associated with the phosphorescence originated from luminescent excimers. Emission from excimers is often observed in organic compounds packed with strong π–π interactions.[42-43] Upon excitation, a molecule in excited state can approach the adjacent one in the ground state, leading to the formation of excimer and consequential excimer luminescence. As shown in Fig. S7, strong π–π interaction is observed between two N–heterocyclic rings from two different AIO clusters, with a displacement angle (θ) of 34 ° and vertical distance (d) of 3.3 Å. These numbers are well within the range of efficient triplet excimer generations.[44]

While the PL lifetimes of compound **2** show very little dependence on temperature, compound **3,** which is made up of the same ligands but involved with coordination of aromatic nitrogen, demonstrates much longer lifetimes and strong temperature dependence. Such differences clearly suggest the significant impact of introducing aromatic units into coordination. The average amplitude-weighted lifetime values of compound **3** decrease from 64.6 μs at 78 K to 13.7 μs at 300 K (Table S2). The PL decay curves at low temperatures (i.e., 78 K and 150 K) are best fit with a monoexponential function, indicating that the emission is purely phosphorescence, coming from the (M+X)LCT excited state. On the other hand, another faster decay component was identified at temperatures above 200 K. Interestingly, as the temperature increases, the fraction of its fast decay rises from 18% at 200 K to 33% at 300 K. This phenomenon is well suited with the thermally activated delayed fluorescence (TADF) mechanism proposed by Yersin et al.[45-46] TADF has been observed in many other CuX–based hybrid materials with small energy differences between the lowest excited singlet state (S_1) and the lowest excited triplet state (T_1).[47-48] A fraction of the electrons can be thermally populated back to S_1 from T_1 through reverse intersystem crossing (RISC) with the energy provided by the increased temperature, thus leading to a S_1 to S_0 radiative transition. The fact that efficient TADF only happens at temperatures above 200 K may indicate a relatively larger energy gap in compound **3**.

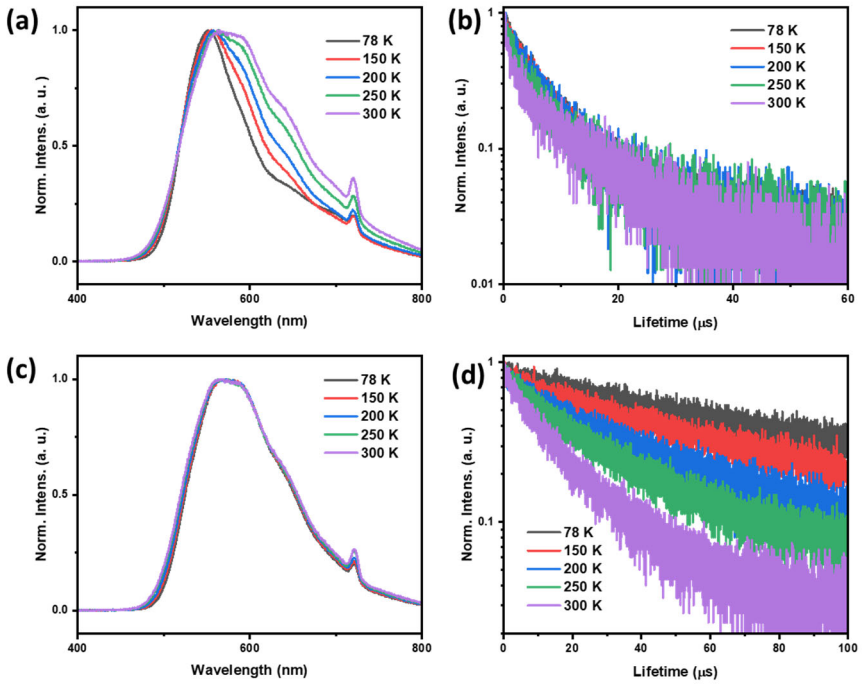

Figure 4. (a) Normalized PL spectra and (b) normalized luminescence decay curves of compound **2** at various temperatures. (c) Normalized PL spectra and (d) normalized luminescence decay curves of compound **3** at various temperatures.

PL decay curves of compound **4** are also best fit with biexponential functions, but with some differences. The fast decay component is extremely sensitive toward temperature changes, as it decreases from 4.81 μs at 78 K to only 52 ns at 300 K. Along with this drastic lifetime change, significant thermal quenching of its emission intensity was observed (Fig. S18), indicative of the CC emission nature of this decay component.[49] Similar properties have been observed in other compounds with CC emissions which is mainly attributed to the thermally facilitated non–radiative pathway.[50] The slow decay component is associated with the (M+X)LCT, confirmed by our DFT calculations. All of these facts suggest that both CC and (M+X)LCT excited states are responsible for the emission of compound **4** and they may be thermally equilibrated with each other.[30, 51-52]

The emission mechanism discussed above are summarized in Fig. S19. Compound **2**, with only aliphatic N to Cu coordination, emits dominantly from ^{3}CC excited state with small contributions from excimers, while compound **3**, in which aromatic N to Cu coordination is also involved, demonstrates emission of both phosphorescence from ^{3}(M+X)LCT and TADF from ^{1}(M+X)LCT. For compound **4**, due to the existence of strong Cu···Cu interactions, both ^{3}CC and ^{3}(M+X)LCT are active, with the former one exhibiting thermally facilitated non–radiative pathway. These results clearly point out that both the ligand configuration and the Cu···Cu distances play important roles in the emission mechanisms of CuX–based hybrid materials.

Conclusion

In summary, a series of AIO-type CuI–based hybrid materials has been synthesized with ligands containing both aromatic and aliphatic coordination sites. Their structures range from 0D molecular species to 2D extended network. Due to the unique interactions at their inorganic/organic interfaces, all title compounds are thermally stable (remaining intact up to 210 °C) and demonstrate good solubility in DMSO, making them suitable for use in solution–processed thin film fabrications. Their emission colors range from cyan (470 nm) to yellow (555 nm) color. The emission mechanisms and effect of ligand hybridization were analyzed by temperature–dependent spectroscopy and theoretical DFT calculations. Overall, this work has provided useful information of the structure–property relationships in CuX–based hybrid materials which may benefit the further development of this promising materials family.

Experimental section

Materials. 1H-benzo[1,2,3]-triazole (99%, Alfa Aesar); 5,6-dimethyl-1H-benzo[d][1,2,3]triazole (99%, Sigma-Aldrich); Formaldehyde (37% in aqueous solution, Alfa Aesar); Thionyl chloride (99%, Alfa Aesar); 1-bromo-2-chloroethane (98%, Alfa Aesar); 1-bromo-3-chloropropane (98%, Alfa Aesar); 1,4-diazabicyclo[2.2.2]octane (98%, TCI); Potassium iodide (99%, Alfa Aesar); Potassium carbonate (99%, TCI); Acetone (99.5%, VWR); Acetonitrile (99.5%, VWR); Ethyl ether (99%, Fisher); Copper iodide (98%, Alfa Aesar); sodium salicylate (99%, Merck).

Preparation of L_1 I. 5,6-dimethyl-1H-benzo[d][1,2,3]triazole (1.47 g, 10 mmol) was dissolved in acetonitrile (100 ml), and then K_2CO_3 (3.3 g, 20 mmol), 1-bromo-2-chloroethane (1 ml, 12 mmol) were added to the reaction at room temperature. After stirred for 3 days, the reaction was filtered, and the filtrate was evaporated under reduced pressure. Purifying with column chromatography gives white solid as 1-(2-chloroethyl)-5,6-dimethyl-1H-benzo[d][1,2,3]triazole (*Cl-dmbt*). *Cl-dmbt* (1.05 g, 5 mmol) and KI (1.6 g, 10 mmol) were added with 20 ml acetone and stirred for 5 h at room temperature before drying under reduced pressure. The solid residue was wash with EtOAc, filtered to obtain filtrate. After removal of the solvent under reduced pressure, MeCN (50 ml) and 1,4-diazabicyclo[2.2.2]octane (0.56 g, 5 mmol) were added and stirring under 60 °C for 2 days. The reaction mixture was evaporated under reduced pressure, washed with ethyl ether and dried under vacuum. Recyclizing with EtOH gives the final product as white solid. The yield of last step is 54%.

Preparation of L_2 I. L_2 I was prepared with a similar procedure as L_1 I but using 1H-benzo[1,2,3]-triazole and 1-bromo-3-chloropropane. White solid was obtained as final product. The yield is 51%.

Preparation of L_3 I. 1-(Chloromethyl)-1H-benzo[d][1,2,3]-triazole (*Cl-mbt*) was prepared according to the reported procedures. The reaction of *Cl-mbt* and 1,4-diazabicyclo[2.2.2]octane follow the same procedure described for L_1 I. Final product was obtained as white solid. The yield is 61%.

Preparation of L_4 I. L_4 I was prepared with a similar procedure as L_1 I but using benzimidazole. Final product is white solid. The yield is 48%.

Synthesis of compound 1. CuI (19 mg, 0.1 mmol) was first dissolved in KI saturated solution (1 ml) in a reaction vial. MeCN (1 ml) was added slowly as another layer, followed by the slow addition of L_1 I (63 mg, 0.15 mmol) MeOH solution (1 ml). The reaction was kept undisturbed at 60 °C for 2 days to yield block-like colourless crystals. The yield is 67% based on CuI.

Synthesis of compound 2. Compound **2** was synthesized in the same way as that of compound **1**, using L_2 I as ligand. The CuI to ligand ratio is 2 to 1. Rod-like colourless crystals were collected by filtration. The yield is 62% based on CuI.

Synthesis of compound 3. Compound **3** was synthesized in the same way as that of compound **3**, using L_2 I as ligand. The CuI to ligand ratio is 1 to 2. Block-like yellow crystals were obtained. The yield is 56% based on CuI.

Synthesis of compound 4. Compound **4** was synthesized in the same way as that of compound **1**, using L_3 I as ligand. The CuI to ligand ratio is 3 to 1. Needle-like yellow crystals were obtained. The yield is 52% based on CuI.

Synthesis of compound 5. Compound **5** was synthesized in the same way as that of compound **1**, using L_4 I as ligand. Plate-like colourless crystals were obtained by filtration. The yield is 44% based on CuI.

Characterizations. Single Crystal X-ray Diffraction (SCXRD) were performed using a D8 goniostat equipped with a Bruker PHOTON100 CMOS detector at the Advanced Light Source (ALS) using synchrotron radiation. The structures were solved by direct methods and refined by full-matrix least-squares on F^2 using the Bruker SHELXTL package. The structures were deposited in Cambridge Crystallographic Data Center (CCDC) with numbers 2233302-2233306. Powder X-ray diffraction (PXRD) analysis was carried out on a Rigaku Ultima-IV unit using Cu $K\alpha_1$ radiation (λ = 1.5406 Å) and a scan speed of 2 °/min. Thermogravimetric analysis (TGA) were performed using the TA Instrument Q5000IR thermogravimetric analyzer with nitrogen flow and sample purge rates at 10 and 25 ml/min, respectively. Optical absorption spectra were measured at room temperature on a Shimadzu UV-3600 UV–vis–NIR spectrometer. The reflectance data were converted to

Kubelka–Munk function. Room temperature PL measurements were carried out on a Horiba Duetta fluorescence spectrophotometer at room temperature. Excitation spectra were measured and monitored at the emission wavelength of maximum intensity. Temperature dependent PL spectra and time-resolved PL decays were recorded on a home-built time-correlated single photon counting instrument with decays recorded in at least 1000 channels using a 410 nm long path filter. PL decays were individually fit with the Fluofit Picoquant software. Internal quantum yield (IQY) was recorded using a C9920-02 absolute quantum yield measurement system (Hamamatsu Photonics). The density of states of selected compounds was calculated using the Cambridge Serial Total Energy Package (CASTEP). Generalized gradient approximations (GGA) with Perdew-Burke-Ernzerhof (PBE) exchange correlation functional (xc) were used for all calculations. Ultrasoft pseudopotentials were used for all elements, the plane-wave kinetic cutoff and the total energy tolerance was set to be 351 eV and 1×10^{-5} eV/atom, respectively.

Conflicts of interest

There are no conflicts to declare.

Supporting Information

^{1}H NMR spectroscopy, structural plots and crystal images, DFT calculation results, and photophysical properties (PDF)

Acknowledgements

The authors acknowledge the partial support from the U.S. Department of Energy, Office of Science, Office of Basic Energy Sciences (Grant No. DE-SC0019902). This research used the Advanced Light Source (ALS), which is a DOE Office of Science User Facility under contract No. DE-AC02-05CH11231. The temperature dependent luminescence work was carried out at the Center for Functional Nanomaterials, Brookhaven National Laboratory (BNL), which is supported by the U.S. Department of Energy, Office of Basic Energy Sciences, under Contract No. DE-SC0012704.

References

1. Smith, M. D.; Karunadasa, H. I., White-Light Emission from Layered Halide Perovskites. *Acc. Chem. Res.* **2018,** *51* (3), 619-627.

2. Cho, H.; Jeong, S.-H.; Park, M.-H.; Kim, Y.-H.; Wolf, C.; Lee, C.-L.; Heo, J. H.; Sadhanala, A.; Myoung, N.; Yoo, S.; Im, S. H.; Friend, R. H.; Lee, T.-W., Overcoming the electroluminescence efficiency limitations of perovskite light-emitting diodes. *Science* **2015,** *350* (6265), 1222-1225.
3. Zhu, K.; Cheng, Z.; Rangan, S.; Cotlet, M.; Du, J.; Kasaei, L.; Teat, S. J.; Liu, W.; Chen, Y.; Feldman, L. C.; O'Carroll, D. M.; Li, J., A New Type of Hybrid Copper Iodide as Nontoxic and Ultrastable LED Emissive Layer Material. *ACS Energy Lett.* **2021,** *6* (7), 2565-2574.
4. Jeon, N. J.; Noh, J. H.; Yang, W. S.; Kim, Y. C.; Ryu, S.; Seo, J.; Seok, S. I., Compositional engineering of perovskite materials for high-performance solar cells. *Nature* **2015,** *517* (7535), 476-480.
5. Jeon, N. J.; Noh, J. H.; Kim, Y. C.; Yang, W. S.; Ryu, S.; Seok, S. I., Solvent engineering for high-performance inorganic–organic hybrid perovskite solar cells. *Nat. Mater.* **2014,** *13* (9), 897-903.
6. Wang, J.-J.; Chen, C.; Chen, W.-G.; Yao, J.-S.; Yang, J.-N.; Wang, K.-H.; Yin, Y.-C.; Yao, M.-M.; Feng, L.-Z.; Ma, C.; Fan, F.-J.; Yao, H.-B., Highly Luminescent Copper Iodide Cluster Based Inks with Photoluminescence Quantum Efficiency Exceeding 98%. *J. Am. Chem. Soc.* **2020,** *142* (8), 3686-3690.
7. Correia, S. F. H.; de Zea Bermudez, V.; Ribeiro, S. J. L.; André, P. S.; Ferreira, R. A. S.; Carlos, L. D., Luminescent solar concentrators: challenges for lanthanide-based organic–inorganic hybrid materials. *J. Mater. Chem. A* **2014,** *2* (16), 5580-5596.
8. Saparov, B.; Mitzi, D. B., Organic–Inorganic Perovskites: Structural Versatility for Functional Materials Design. *Chem. Rev.* **2016,** *116* (7), 4558-4596.
9. Kobayashi, H.; Cui, H.; Kobayashi, A., Organic Metals and Superconductors Based on BETS (BETS = Bis(ethylenedithio)tetraselenafulvalene). *Chem. Rev.* **2004,** *104* (11), 5265-5288.
10. Yam, V. W.-W.; Au, V. K.-M.; Leung, S. Y.-L., Light-Emitting Self-Assembled Materials Based on d8 and d10 Transition Metal Complexes. *Chem. Rev.* **2015,** *115* (15), 7589-7728.
11. Hei, X.; Li, J., All-in-one: a new approach toward robust and solution-processable copper halide hybrid semiconductors by integrating covalent, coordinate and ionic bonds in their structures. *Chem. Sci.* **2021,** *12* (11), 3805-3817.
12. Baranov, A. Y.; Pritchina, E. A.; Berezin, A. S.; Samsonenko, D. G.; Fedin, V. P.; Belogorlova, N. A.; Gritsan, N. P.; Artem'ev, A. V., Beyond Classical Coordination Chemistry: The First Case of a Triply Bridging Phosphine Ligand. *Angew. Chem. Int. Ed.* **2021,** *60* (22), 12577-12584.
13. Matejdes, M.; Stöter, M.; Czerwieniec, R.; Leitl, M.; Rosenfeldt, S.; Schumacher, T.; Albert, J.; Lippitz, M.; Yersin, H.; Breu, J., Sandwich-Like Encapsulation of a Highly Luminescent Copper(I) Complex. *Adv. Opt. Mater.* **2021,** *9* (19), 2100516.
14. Ford, P. C.; Cariati, E.; Bourassa, J., Photoluminescence Properties of Multinuclear Copper(I) Compounds. *Chem. Rev.* **1999,** *99* (12), 3625-3648.
15. Tsuge, K.; Chishina, Y.; Hashiguchi, H.; Sasaki, Y.; Kato, M.; Ishizaka, S.; Kitamura, N., Luminescent copper(I) complexes with halogenido-bridged dimeric core. *Coord. Chem. Rev.* **2016,** *306*, 636-651.
16. Liu, W.; Fang, Y.; Wei, G. Z.; Teat, S. J.; Xiong, K.; Hu, Z.; Lustig, W. P.; Li, J., A Family of Highly Efficient CuI-Based Lighting Phosphors Prepared by a Systematic, Bottom-up Synthetic Approach. *J. Am. Chem. Soc.* **2015,** *137* (29), 9400-9408.
17. Zhang, X.; Liu, W.; Wei, G. Z.; Banerjee, D.; Hu, Z.; Li, J., Systematic Approach in Designing Rare-Earth-Free Hybrid Semiconductor Phosphors for General Lighting Applications. *J. Am. Chem. Soc.* **2014,** *136* (40), 14230-14236.
18. Liu, W.; Fang, Y.; Li, J., Copper Iodide Based Hybrid Phosphors for Energy-Efficient General Lighting Technologies. *Adv. Funct. Mater.* **2018,** *28* (8), 1705593.

19. Liu, W.; Zhu, K.; Teat, S. J.; Dey, G.; Shen, Z.; Wang, L.; O'Carroll, D. M.; Li, J., All-in-One: Achieving Robust, Strongly Luminescent and Highly Dispersible Hybrid Materials by Combining Ionic and Coordinate Bonds in Molecular Crystals. *J. Am. Chem. Soc.* **2017,** *139* (27), 9281-9290.
20. Yao, J.-S.; Wang, J.-J.; Yang, J.-N.; Yao, H.-B., Modulation of Metal Halide Structural Units for Light Emission. *Acc. Chem. Res.* **2021,** *54* (2), 441-451.
21. Hei, X.; Teat, S. J.; Liu, W.; Li, J., Eco-friendly, solution-processable and efficient low-energy lighting phosphors: copper halide based hybrid semiconductors Cu4X6(L)2 (X = Br, I) composed of covalent, ionic and coordinate bonds. *J. Mater. Chem. C* **2020,** *8* (47), 16790-16797.
22. Hei, X.; Zhu, K.; Carignan, G.; Teat, S. J.; Li, M.; Zhang, G.; Bonite, M.; Li, J., Solution-processable copper(I) iodide-based inorganic-organic hybrid semiconductors composed of both coordinate and ionic bonds. *J. Solid State Chem.* **2022,** *314*, 123427.
23. Hei, X.; Liu, W.; Zhu, K.; Teat, S. J.; Jensen, S.; Li, M.; O'Carroll, D. M.; Wei, K.; Tan, K.; Cotlet, M.; Thonhauser, T.; Li, J., Blending Ionic and Coordinate Bonds in Hybrid Semiconductor Materials: A General Approach toward Robust and Solution-Processable Covalent/Coordinate Network Structures. *J. Am. Chem. Soc.* **2020,** *142* (9), 4242-4253.
24. Li, H.; Lv, Y.; Zhou, Z.; Tong, H.; Liu, W.; Ouyang, G., Coordinated Anionic Inorganic Module—An Efficient Approach Towards Highly Efficient Blue-Emitting Copper Halide Ionic Hybrid Structures. *Angew. Chem. Int. Ed.* **2022,** *61* (8), e202115225.
25. Fang, Y.; Liu, W.; Teat, S. J.; Dey, G.; Shen, Z.; An, L.; Yu, D.; Wang, L.; O'Carroll, D. M.; Li, J., A Systematic Approach to Achieving High Performance Hybrid Lighting Phosphors with Excellent Thermal- and Photostability. *Adv. Funct. Mater.* **2017,** *27* (3), 1603444.
26. Pfrunder, M. C.; Micallef, A. S.; Rintoul, L.; Arnold, D. P.; Davy, K. J. P.; McMurtrie, J., Exploitation of the Menshutkin Reaction for the Controlled Assembly of Halogen Bonded Architectures Incorporating 1,2-Diiodotetrafluorobenzene and 1,3,5-Triiodotrifluorobenzene. *Cryst. Growth Des.* **2012,** *12* (2), 714-724.
27. Hei, X.; Fang, Y.; Teat, S. J.; Farrington, C.; Bonite, M.; Li, J., Copper(I) iodide-based organic–inorganic hybrid compounds as phosphor materials. *Z. Naturforsch. B* **2021,** *76* (10-12), 759-764.
28. Liu, W.; Banerjee, D.; Lin, F.; Li, J., Strongly luminescent inorganic–organic hybrid semiconductors with tunable white light emissions by doping. *J. Mater. Chem. C* **2019,** *7* (6), 1484-1490.
29. Bondi, A., van der Waals Volumes and Radii. *J. Phys. Chem.* **1964,** *68* (3), 441-451.
30. Artem'ev, A. V.; Davydova, M. P.; Hei, X.; Rakhmanova, M. I.; Samsonenko, D. G.; Bagryanskaya, I. Y.; Brylev, K. A.; Fedin, V. P.; Chen, J.-S.; Cotlet, M.; Li, J., Family of Robust and Strongly Luminescent CuI-Based Hybrid Networks Made of Ionic and Dative Bonds. *Chem. Mater.* **2020,** *32* (24), 10708-10718.
31. Fang, Y.; Zhu, K.; Teat, S. J.; Reid, O. G.; Hei, X.; Zhu, K.; Fang, X.; Li, M.; Sojdak, C. A.; Cotlet, M.; Li, J., Robust and Highly Conductive Water-Stable Copper Iodide-Based Hybrid Single Crystals. *Chem. Mater.* **2022**.
32. Ki, W.; Hei, X.; Yi, H. T.; Liu, W.; Teat, S. J.; Li, M.; Fang, Y.; Podzorov, V.; Garfunkel, E.; Li, J., Two-Dimensional Copper Iodide-Based Inorganic–Organic Hybrid Semiconductors: Synthesis, Structures, and Optical and Transport Properties. *Chem. Mater.* **2021,** *33* (13), 5317-5325.
33. Clark, S. J.; Segall, M. D.; Pickard, C. J.; Hasnip, P. J.; Probert, M. J.; Refson, K.; Payne, M. C., First principles methods using CASTEP. *Z. Kristallogr. Cryst. Mater.* **2005,** *220* (5-6), 567-570.
34. Benito, Q.; Le Goff, X. F.; Nocton, G.; Fargues, A.; Garcia, A.; Berhault, A.; Kahlal, S.; Saillard, J.-Y.; Martineau, C.; Trébosc, J.; Gacoin, T.; Boilot, J.-P.; Perruchas, S., Geometry Flexibility of Copper Iodide Clusters: Variability in Luminescence Thermochromism. *Inorg. Chem.* **2015,** *54* (9), 4483-4494.

35. Song, K.-H.; Wang, J.-J.; Feng, L.-Z.; He, F.; Yin, Y.-C.; Yang, J.-N.; Song, Y.-H.; Zhang, Q.; Ru, X.-C.; Lan, Y.-F.; Zhang, G.; Yao, H.-B., Thermochromic Phosphors Based on One-Dimensional Ionic Copper-Iodine Chains Showing Solid-State Photoluminescence Efficiency Exceeding 99 %. *Angew. Chem. Int. Ed.* **2022,** *61* (38), e202208960.
36. Wei, Q.; Chang, T.; Zeng, R.; Cao, S.; Zhao, J.; Han, X.; Wang, L.; Zou, B., Self-Trapped Exciton Emission in a Zero-Dimensional (TMA)2SbCl5·DMF Single Crystal and Molecular Dynamics Simulation of Structural Stability. *J. Phys. Chem. Lett.* **2021,** *12* (30), 7091-7099.
37. Zhou, C.; Lin, H.; Tian, Y.; Yuan, Z.; Clark, R.; Chen, B.; van de Burgt, L. J.; Wang, J. C.; Zhou, Y.; Hanson, K.; Meisner, Q. J.; Neu, J.; Besara, T.; Siegrist, T.; Lambers, E.; Djurovich, P.; Ma, B., Luminescent zero-dimensional organic metal halide hybrids with near-unity quantum efficiency. *Chem. Sci.* **2018,** *9* (3), 586-593.
38. Li, M.; Xia, Z., Recent progress of zero-dimensional luminescent metal halides. *Chem. Soc. Rev.* **2021,** *50* (4), 2626-2662.
39. Hao, P.; Qiao, Y.; Yu, T.; Shen, J.; Liu, F.; Fu, Y., Three iodocuprate hybrids symmetrically modulated by positional isomers and the chiral conformation of N-benzyl-methylpyridinium. *RSC Adv.* **2016,** *6* (58), 53566-53572.
40. Shen, J.-J.; Li, X.-X.; Yu, T.-L.; Wang, F.; Hao, P.-F.; Fu, Y.-L., Ultrasensitive Photochromic Iodocuprate(I) Hybrid. *Inorg. Chem.* **2016,** *55* (17), 8271-8273.
41. Artem'ev, A. V.; Pritchina, E. A.; Rakhmanova, M. I.; Gritsan, N. P.; Bagryanskaya, I. Y.; Malysheva, S. F.; Belogorlova, N. A., Alkyl-dependent self-assembly of the first red-emitting zwitterionic {Cu4I6} clusters from [alkyl-P(2-Py)3]+ salts and CuI: when size matters. *Dalton Trans.* **2019,** *48* (7), 2328-2337.
42. Birks, J. B., Excimers. *Rep. Prog. Phys.* **1975,** *38* (8), 903.
43. Chen, Y.-H.; Tang, K.-C.; Chen, Y.-T.; Shen, J.-Y.; Wu, Y.-S.; Liu, S.-H.; Lee, C.-S.; Chen, C.-H.; Lai, T.-Y.; Tung, S.-H.; Jeng, R.-J.; Hung, W.-Y.; Jiao, M.; Wu, C.-C.; Chou, P.-T., Insight into the mechanism and outcoupling enhancement of excimer-associated white light generation. *Chem. Sci.* **2016,** *7* (6), 3556-3563.
44. Liu, Z.; Tian, Y.; Yang, J.; Li, A.; Wang, Y.; Ren, J.; Fang, M.; Tang, B. Z.; Li, Z., Direct demonstration of triplet excimer in purely organic room temperature phosphorescence through rational molecular design. *Light Sci. Appl.* **2022,** *11* (1), 142.
45. Leitl, M. J.; Krylova, V. A.; Djurovich, P. I.; Thompson, M. E.; Yersin, H., Phosphorescence versus Thermally Activated Delayed Fluorescence. Controlling Singlet–Triplet Splitting in Brightly Emitting and Sublimable Cu(I) Compounds. *J. Am. Chem. Soc.* **2014,** *136* (45), 16032-16038.
46. Czerwieniec, R.; Leitl, M. J.; Homeier, H. H. H.; Yersin, H., Cu(I) complexes – Thermally activated delayed fluorescence. Photophysical approach and material design. *Coord. Chem. Rev.* **2016,** *325*, 2-28.
47. Yang, Y.; Li, N.; Miao, J.; Cao, X.; Ying, A.; Pan, K.; Lv, X.; Ni, F.; Huang, Z.; Gong, S.; Yang, C., Chiral Multi-Resonance TADF Emitters Exhibiting Narrowband Circularly Polarized Electroluminescence with an EQE of 37.2. *Angew. Chem. Int. Ed.* **2022,** *61* (30), e202202227.
48. Klein, M.; Rau, N.; Wende, M.; Sundermeyer, J.; Cheng, G.; Che, C.-M.; Schinabeck, A.; Yersin, H., Cu(I) and Ag(I) Complexes with a New Type of Rigid Tridentate N,P,P-Ligand for Thermally Activated Delayed Fluorescence and OLEDs with High External Quantum Efficiency. *Chem. Mater.* **2020,** *32* (24), 10365-10382.
49. Morad, V.; Yakunin, S.; Benin, B. M.; Shynkarenko, Y.; Grotevent, M. J.; Shorubalko, I.; Boehme, S. C.; Kovalenko, M. V., Hybrid 0D Antimony Halides as Air-Stable Luminophores for High-Spatial-Resolution Remote Thermography. *Adv. Mater.* **2021,** *33* (9), 2007355.

50. Yakunin, S.; Benin, B. M.; Shynkarenko, Y.; Nazarenko, O.; Bodnarchuk, M. I.; Dirin, D. N.; Hofer, C.; Cattaneo, S.; Kovalenko, M. V., High-resolution remote thermometry and thermography using luminescent low-dimensional tin-halide perovskites. *Nat. Mater.* **2019,** *18* (8), 846-852.
51. Ford, P. C.; Vogler, A., Photochemical and photophysical properties of tetranuclear and hexanuclear clusters of metals with d10 and s2 electronic configurations. *Acc. Chem. Res.* **1993,** *26* (4), 220-226.
52. Liu, Z.; Djurovich, P. I.; Whited, M. T.; Thompson, M. E., Cu4I4 Clusters Supported by P∧N-type Ligands: New Structures with Tunable Emission Colors. *Inorg. Chem.* **2012,** *51* (1), 230-236.

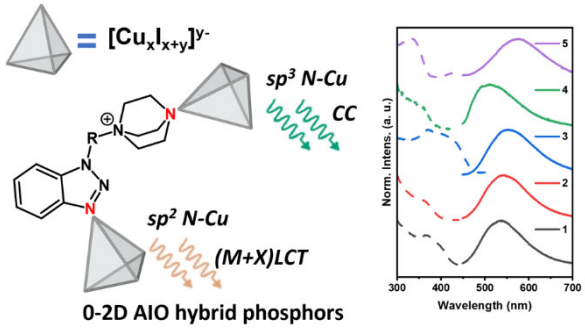

For Table of Contents Only

Synopsis: A series of All-In-One type CuI based hybrid materials consisting of cationic ligands with both aromatic and aliphatic coordination sites. Their structures range from oD molecular species to 2D extended network. These compounds demonstrate good thermal stability, solubility in DMSO and photoluminescence. The emission mechanisms and effect of ligand hybridization were analyzed, providing useful information of the structure–property relationships in CuX–based hybrid materials.